

PAPER • OPEN ACCESS

## Elastic Magnetic Electron Scattering from odd-A Nuclei

To cite this article: P. Sarriguren *et al* 2020 *J. Phys.: Conf. Ser.* **1555** 012001

View the [article online](#) for updates and enhancements.



**IOP | ebooks™**

Bringing together innovative digital publishing with leading authors from the global scientific community.

Start exploring the collection—download the first chapter of every title for free.

# Elastic Magnetic Electron Scattering from odd-A Nuclei

P. Sarriguren<sup>1</sup>, O. Moreno<sup>2</sup>, E. Moya de Guerra<sup>2</sup>, D.N. Kadrev<sup>3</sup>,  
A.N. Antonov<sup>3</sup>, and M.K. Gaidarov<sup>3</sup>

<sup>1</sup> Instituto de Estructura de la Materia, IEM-CSIC, Serrano 123, E-28006 Madrid, Spain

<sup>2</sup> Departamento de Estructura de la Materia, Física Térmica y Electrónica, Facultad de Ciencias Físicas, Universidad Complutense de Madrid, Madrid E-28040, Spain

<sup>3</sup> Institute for Nuclear Research and Nuclear Energy, Bulgarian Academy of Sciences, Sofia 1784, Bulgaria

E-mail: p.sarriguren@csic.es

## Abstract.

Magnetic form factors from odd- $A$  spherical and deformed nuclei corresponding to elastic electron scattering are calculated in the plane-wave Born approximation. The nuclear structure of the target is described within a deformed self-consistent mean-field calculation with effective interactions of Skyrme type and pairing correlations in the BCS approximation. We focus our attention to stable nuclei where experimental information is available. It is shown that the deformed formalism improves the agreement with experiment in deformed nuclei, while reproducing equally well spherical nuclei by taking properly the spherical limit of the deformed model. Effects of the collective rotation and nucleon-nucleon correlations are also studied. These results demonstrate the ability of the method to address electron scattering from unstable nuclei to be measured in future experiments on electron-ion beam colliders.

## 1. Introduction

Electron scattering has been shown in the past to be a powerful tool for studying the electromagnetic properties of nuclei. The elastic, inelastic, and quasielastic regimes have been explored, providing us with the most accurate measurements on charge distributions and radii, transition probabilities, as well as momentum distributions and spectroscopic factors [1, 2, 3]. The main advantages of using electrons as probes are due to the characteristics of the electromagnetic interaction, which is accurately described by quantum electrodynamics. The weakness of the interaction allows one to describe the scattering process in first order perturbation within the one-photon exchange approximation. In addition, the energy and momentum transferred by the virtual photon exchanged in the process can be varied independently, mapping out the Fourier transform of the densities.

However, electron scattering is not only sensitive to the nuclear charge distribution. Electrons also scatter from the nuclear electromagnetic current distributions, giving us information on the convection and magnetization currents within the nucleus. In particular, elastic magnetic electron scattering is a source of information on those nuclear ground-state distributions [4, 5].



Content from this work may be used under the terms of the [Creative Commons Attribution 3.0 licence](https://creativecommons.org/licenses/by/3.0/). Any further distribution of this work must maintain attribution to the author(s) and the title of the work, journal citation and DOI.

Magnetic scattering shares the advantages of the electromagnetic probes, but there are also significant differences as compared to charge scattering. Because the angular momenta of the nucleons pair off within the core, the magnetic properties in odd- $A$  nuclei are determined to a large extent by the unpaired nucleon. Therefore, magnetic electron scattering would provide information on the single-particle properties of the valence nuclear wave function. Since the intrinsic magnetic moments of protons and neutrons are similar in magnitude, magnetic electron scattering will provide information on both nucleons, contrary to the case of charge scattering which is mostly sensitive to protons. Similarly to the case of charge scattering, magnetic scattering has been also studied in stable nuclei from different theoretical formalisms [4], including the shell model [6], relativistic mean field [7], and deformed mean field models [5, 8, 9, 10, 11].

Electron scattering experiments have been limited so far to stable isotopes, but the advantages of electron probes mentioned above can be exploited to gain information on unstable nuclei as well. New interesting and challenging properties like nuclear halos, neutron skins, or the evolution of the charge distributions in isotopic chains will be addressed at new facilities [12, 13], such as ELISE (FAIR-GSI) and SCRIT (RIKEN). These experiments will test different theoretical models. Examples of these studies can be found in Refs. [14, 15, 16, 17, 18]. Electron scattering experiments are also used as an additional tool to complement the information obtained by other probes. This is the case of magnetic dipole excitations in nuclei, where it is well known [19, 20] that complementary information is obtained when using different electromagnetic ( $\gamma, \gamma'$ ), ( $e, e'$ ) or hadronic ( $p, p'$ ) probes.

In this work we analyze the dependence on deformation of the magnetic form factors of odd- $A$  nuclei and we show the capability of the deformed formalism to describe both spherical and deformed nuclei. To fulfill this purpose, we compare our results with the available experimental information on stable nuclei.

## 2. Theoretical Formalism

The formalism of electron scattering from deformed nuclei followed in this work was introduced and discussed in Refs. [5, 8]. The method was already applied to different cases [9, 10, 11, 21, 22], where the various sensitivities of the results to different approximations concerning nuclear structure and reaction mechanism were studied. In particular, it was shown that the magnetic form factors of deformed nuclei may differ considerably from those of spherical nuclei. Here, we briefly summarize this formalism. Following the notation of Ref. [5], the general cross section for electron scattering of ultrarelativistic electrons for transitions from the nuclear ground state ( $I_i$ ) to final states ( $I_f$ ) is given in the plane-wave Born approximation (PWBA) by

$$\left. \frac{d\sigma}{d\Omega} \right|_{I_i \rightarrow I_f} = 4\pi\sigma_M f_{\text{rec}}^{-1} \left[ V_L |F_L|^2 + V_T |F_T|^2 \right], \quad (1)$$

in terms of the Mott cross section  $\sigma_M$  and a recoil factor  $f_{\text{rec}}$ . The cross section is separated into longitudinal or Coulomb (L) and transverse (T) contributions, weighted with different kinematical factors,

$$V_L = (Q^2/q^2)^2, \quad V_T = \tan^2(\theta/2) - (Q^2/2q^2), \quad (2)$$

where the kinematical variables are defined so that an incident electron with four-momentum  $k_{i\mu} = (\epsilon_i, \mathbf{k}_i)$  is scattered through an angle  $\theta$  to four-momentum  $k_{f\mu} = (\epsilon_f, \mathbf{k}_f)$  by exchanging a virtual photon with four-momentum  $Q = (\omega, \mathbf{q})$ .

Because all the charged nucleons contribute equally to the Coulomb (charge) form factors  $F_L$ , they scale like  $Z^2$  in the cross section. On the other hand, transverse form factors  $F_T$  are basically single-particle observables that depend mostly on the properties of the unpaired

nucleon in the outermost shell. As a consequence,  $F_L$  dominates at most angles and special kinematic conditions are needed to maximize magnetic  $F_T$  contributions. This is why backward scattering ( $\theta = 180^\circ$ ) is commonly used to measure  $F_T$ .

The dependence on the nuclear structure is contained in the  $q$ -dependent L and T form factors, which are written in terms of Coulomb (C), transverse electric (E), and transverse magnetic (M) multipoles,

$$|F_L|^2 = \sum_{\lambda \geq 0} |F^{C\lambda}|^2, \quad |F_T|^2 = \sum_{\lambda \geq 1} \left[ |F^{M\lambda}|^2 + |F^{E\lambda}|^2 \right], \quad (3)$$

which are defined as the reduced matrix elements of the corresponding multipole operators  $\hat{T}^{\sigma\lambda}$  between initial and final nuclear states

$$|F^{\sigma\lambda}|^2 = \frac{|\langle I_f || \hat{T}^{\sigma\lambda}(q) || I_i \rangle|^2}{2I_i + 1}. \quad (4)$$

For elastic scattering, parity and time reversal invariance imply that only the even Coulomb and odd transverse magnetic multipoles contribute. Then, at  $\theta = 180^\circ$  only odd magnetic multipoles will survive in PWBA,

$$\left. \frac{d\sigma}{d\Omega} \right|_{I_i \rightarrow I_f} = 4\pi \sigma_M f_{\text{rec}}^{-1} V_T |F_T|^2, \quad |F_T(q)|^2 = \sum_{\lambda=\text{odd}} |F^{M\lambda}|^2. \quad (5)$$

The magnetic multipole operators are defined as

$$\hat{T}_\mu^{M\lambda}(q) = i^\lambda \int d\mathbf{r} j_\lambda(qr) \mathbf{Y}_{\lambda\lambda}^\mu(\Omega_r) \cdot \hat{\mathbf{J}}(\mathbf{r}), \quad (6)$$

where  $\hat{\mathbf{J}}(\mathbf{r})$  is the current density operator that contains both convection and magnetization components arising from the motion and from the intrinsic magnetic moments of the nucleons, respectively. When we calculate the total form factors, we include standard center of mass and finite nucleon size corrections [11].

The effects of Coulomb distortion can be quantitatively taken into account within the distorted-wave Born approximation (DWBA) [23]. Nevertheless, for the analysis of experimental data on magnetic scattering, PWBA is commonly used. This is because in PWBA the connection between the data and the underlying physical quantities is more transparent, and calculations are much simpler. The most important effect of the Coulomb distortion can be accounted for by using an effective momentum transfer. This procedure was done in the data used in this work (taken from Ref. [4]), where the experimental form factors were converted into plane-wave form factors that can be directly compared with PWBA calculations.

The ground state of an axially symmetric deformed nucleus is characterized by its angular momentum  $I$ , projection along the symmetry axis  $k$ , and parity  $\pi$ . The magnetic  $F^{M\lambda}$  multipole form factors can be written in terms of intrinsic form factors  $\mathcal{F}^{M\lambda}$ , weighted by angular momentum dependent coefficients, that depend only on the intrinsic structure of the ground-state band [5]. The transition multipoles in Eq. (5) for the elastic case  $I_f = I_i = k$  can be written as

$$F^{M\lambda} \Big|_{\text{def}} = \langle k k \lambda 0 | k k \rangle \mathcal{F}_k^{M\lambda} + \langle k -k \lambda 2k | k k \rangle \mathcal{F}_{2k}^{M\lambda} + \frac{\lambda(\lambda+1)}{\sqrt{2}} \langle k k \lambda 0 | k k \rangle \mathcal{F}_R^{M\lambda}, \quad (7)$$

where  $\mathcal{F}_R^{M\lambda}$  are the rotational multipoles that depend on the nuclear rotational model used to describe the band [5]. The single-particle multipoles  $\mathcal{F}_k^{M\lambda}$  and  $\mathcal{F}_{2k}^{M\lambda}$  depend only on the single-particle intrinsic wave function of the odd nucleon. They are different from zero only for  $k \neq 0$  bands and are given by,

$$\mathcal{F}_k^{M\lambda} = \langle \phi_k | \hat{T}_0^{M\lambda} | \phi_k \rangle, \quad \mathcal{F}_{2k}^{M\lambda} = \langle \phi_k | \hat{T}_{2k}^{M\lambda} | \phi_{\bar{k}} \rangle + \delta_{k,1/2} \frac{a}{\sqrt{2}} \mathcal{F}_R^{M\lambda}. \quad (8)$$

$\phi_k$  and  $\phi_{\bar{k}}$  are the wave functions of the odd nucleon and its time reverse, respectively, and  $a = \langle \phi_k | j_+ | \phi_{\bar{k}} \rangle$  is the decoupling parameter for  $k = 1/2$  bands.

In the HF+BCS method for axially symmetric deformed nuclei [24], the wave functions are expanded into the eigenfunctions of an axially deformed harmonic oscillator potential, using 11 major shells. In the present work, the mean field of the odd- $A$  nucleus is generated within the equal filling approximation, a prescription used in self-consistent mean-field calculations that preserves time-reversal invariance. The odd nucleon orbital is chosen according to the experimental spin and parity values. All the results presented in this work correspond to the Skyrme interaction SLy4 [25].

The explicit expressions for the intrinsic single-particle and rotational form factors in Eqs.(8) in terms of the intrinsic wave functions can be found in Refs. [5, 8], where the multipoles  $\mathcal{F}_R^{M\lambda}$  are given for different microscopic (Projected Hartree-Fock and cranking), as well as macroscopic (rigid rotor and irrotational flow) models.

In the spherical limit, the single-particle wave functions contain a single angular momentum component. In this limit there are no collective magnetic multipoles ( $\mathcal{F}_R^{M\lambda} = 0$ ). The deformed form factor and its spherical limit are related with Clebsch-Gordan geometrical factors [11],

$$F^{M\lambda} \Big|_{\text{sph limit}} = \frac{F^{M\lambda} \Big|_{\text{def}}}{\langle jj\lambda 0 | jj \rangle^2 \left[ 1 + \delta_{\lambda,2j} \frac{\langle j -j \lambda 2j | jj \rangle^2}{\langle jj\lambda 0 | jj \rangle^2} \right]}. \quad (9)$$

It is also well known [26, 27] that many experimental data of scattering and reactions on nuclei show the existence of sizable nucleon-nucleon (NN) correlation effects on nuclear properties that cannot be described correctly within the mean-field approximation. But it is still possible to restore the single-particle picture in more general methods that include NN correlations by using the so-called natural orbitals (NOs) and natural occupation probabilities, associated to the one-body density matrix (OBDM) that corresponds to the correlated ground state of the system. The NOs and the natural occupation numbers are obtained by diagonalizing the OBDM, which in the present work, is obtained within the Coherent Density Fluctuation Model (CDFM) [26, 27]. They are used in the calculations of the magnetic form factors.

### 3. Results

We have chosen for this study several nuclei  $^{17}\text{O}$ ,  $^{25}\text{Mg}$ ,  $^{41}\text{Ca}$ , and  $^{59}\text{Co}$  for which experimental information on elastic magnetic electron scattering form factors is available. Therefore, we can test the reliability of the theoretical models. First, we study two spherical nuclei,  $^{17}\text{O}$  and  $^{41}\text{Ca}$ .

In Figures 1 and 2 we show in the top panels the magnetic form factors from the deformed model in the spherical limit defined by Eq. (9). The bottom panels show a comparison between the results in the spherical limit (sph limit) with the results obtained from a standard spherical calculation (st sph) based on the code by H. P. Blok and J. H. Heisenberg [28]. This comparison helps us to check the reliability of the spherical limit. We also study the role of NN correlations (st sph + CDFM) by including these effects and comparing the results. We can see from the figures that correlations beyond the mean-field picture are needed to account for the behavior at high momentum transfer and that the NO representation is a convenient way to deal with these correlations. Data are taken from the compilation made in Ref. [4].

Figure 1 for  $^{17}\text{O}$  ( $I^\pi = 5/2^+$ ) shows the first example of this comparison. The first peak is due to the M1 multipole, while the second peak and the tail at large  $q$  are determined by the M5 multipole. The contribution from the M3 multipole appears in the middle part at around  $1 \text{ fm}^{-1}$ . The agreement between the results from the spherical limit and the results from the

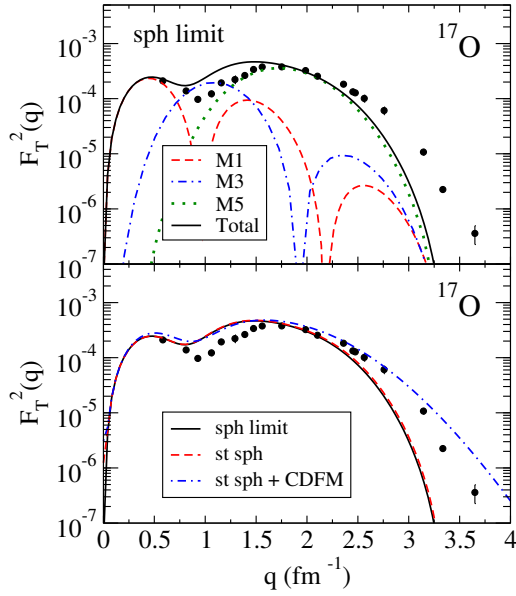


**Figure 1.** Magnetic form factors of  $^{17}\text{O}$  decomposed into M1, M3, and M5 multipoles in the spherical limit (top). Comparison between the spherical limit and the standard spherical calculation alone and together with CDFM (bottom).

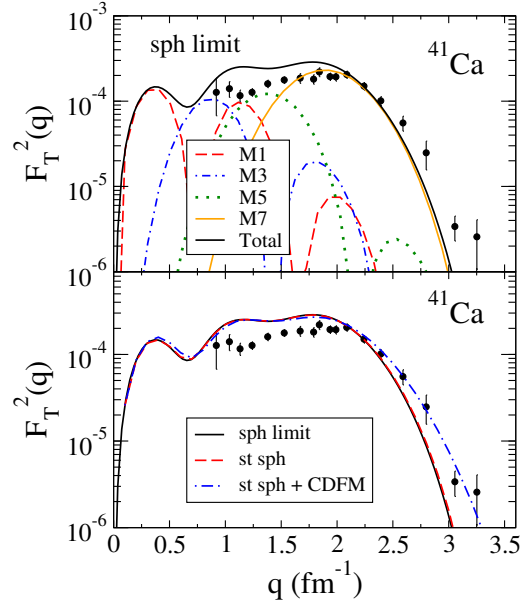


**Figure 2.** Same as in Figure 1, but for the spherical nucleus  $^{41}\text{Ca}$  decomposed into M1, M3, M5, and M7 multipoles.

standard spherical calculation [28] is remarkable and this is the general result observed in all cases studied. The main effect of the NN correlations calculated with natural orbits within the CDFM [27] is to modify the tails by shifting the form factors to higher  $q$ -values, thus improving the agreement with experiment. This feature is also observed in all cases studied. In Figure 2 we show the results for  $^{41}\text{Ca}$  ( $I^\pi = 7/2^-$ ). M1 (M7) determines the low (high)  $q$  behavior, while M3 and M5 fill the region between  $0.5 < q < 1.5 \text{ fm}^{-1}$ . The tails are again improved when NN correlations are included.

In Figures 3 and 4, we compare in the top panels calculations from the deformed and spherical formalisms in the case of the deformed nuclei  $^{25}\text{Mg}$  and  $^{59}\text{Co}$ . In this case, to calculate the spherical limit, a HF+BCS calculation constrained to zero deformation has been performed for each nucleus. The bottom panels show the total magnetic form factor from the deformed model decomposed into multipoles with both single-particle and rotational collective contributions from the core  $\mathcal{F}_R^{M\lambda}$ , calculated in the cranking model.

Figure 3 shows the results for  $^{25}\text{Mg}$  ( $I^\pi = 5/2^+$ ). In the top panel we show the deformed calculations compared with the spherical limit, as well as with the standard spherical calculation with CDFM correlations. We observe in the deformed case a clear improvement of the agreement with experiment. The first peak is due to M1, whereas the second is due to M5, with a negligible contribution from M3. The contribution of the core rotational currents appears mainly in the first peak, due to the effect on M1 at low  $q$ . This contribution improves the agreement in the first peak. The high  $q$  behavior is determined by the M5 multipole, which is practically unaffected by  $\mathcal{F}_R^{M5}$ . Figure 4 displays the results for the nucleus  $^{59}\text{Co}$  ( $I^\pi = 7/2^-$ ). The data are somewhat better reproduced by the spherical case at low and high  $q$  values, but the deformed calculations reproduce better the whole structure of the first peak including the fall of the curve. This could be an indication that we are dealing in this case with small deformations. However, the filling

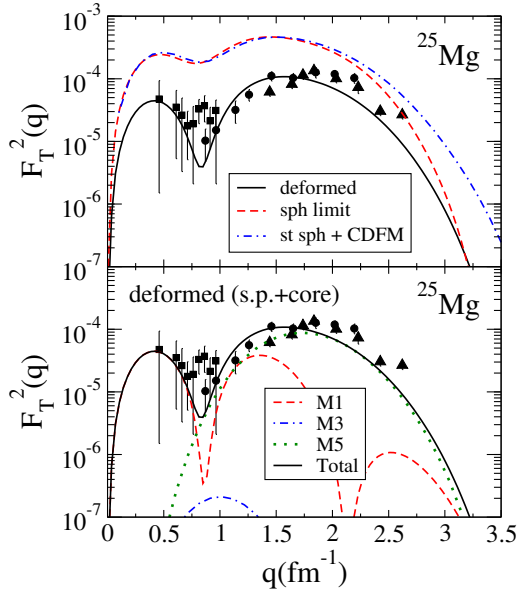


**Figure 3.** Magnetic form factors of  $^{25}\text{Mg}$  in the deformed formalism and in its spherical limit (top). Multipole decomposition of the deformed form factor including collective contributions (bottom).

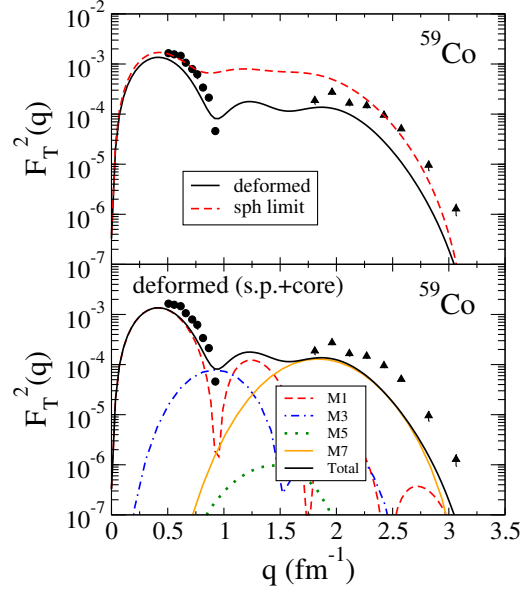


**Figure 4.** Same as in Figure 3, but for  $^{59}\text{Co}$ .

of the form factors in the range  $1 < q < 2 \text{ fm}^{-1}$  produced by the spherical calculation is not observed experimentally, thus favoring the deformed picture.

#### 4. Conclusions

In this work we have calculated magnetic form factors in elastic electron scattering from odd- $A$  nuclei within PWBA and within a deformed formalism for the nuclear structure, using wave functions obtained from self-consistent HF+BCS calculations with Skyrme forces.

We have recovered the spherical limit of these calculations and have compared the results with those obtained from purely spherical codes, finding a perfect agreement. The spherical formalism reproduces quite reasonably the main features of the elastic magnetic form factors measured in spherical nuclei. NN correlations are included with natural orbits within the CDFM and are found to shift the tails of the form factors to higher momentum transfer, improving the agreement with experiment.

Then, we proceed to calculate deformed nuclei and compare both spherical and deformed calculations with experiment. The deformed picture improves the agreement with the data. It is found that in odd- $A$  deformed nuclei, the main contribution to the magnetic form factor comes from the odd particle. This result is in contrast to the case of charge form factors, where all the nucleons contribute significantly. The collective effects in the deformed formulation show up through changes in the single-particle wave functions, in the explicit contribution of rotational multipoles  $\mathcal{F}_R^{M\lambda}$ , as well as in the geometrical factors that reduce the multipoles with respect to the spherical ones and help to improve the agreement with experiment in all the deformed cases studied. The effect of the rotational multipoles is more important in the low- $q$  region ( $q < 1 \text{ fm}^{-1}$ ), where they interfere with the single-particle contributions.

We have shown that we can deal with spherical and deformed isotopes in a unified way

using the same methods and codes. It is also worth noting that, at variance with the approach followed in other works [16, 7], in this paper there is no fit of the coefficients weighting the various multipoles contributing to the total magnetic form factors. In the present formalism, the weights of the multipoles are directly given by the geometrical factors relating the intrinsic with the transition multipoles and therefore we do not introduce any adjustable parameter. Once the capability of the model has been tested against data on magnetic form factors on spherical and deformed stable nuclei, we have a trustable formalism to explore the predictions on unstable nuclei.

## Acknowledgments

This work was supported by MCIU/AEI/FEDER,UE (Spain) under Contract No. PGC2018-093636-B-I00. Three of the authors (DNK, ANA, and MKG) are grateful for support of the Bulgarian Science Fund under Contract No. DFNI-T02/19.

## References

- [1] Donnelly TW and Walecka JD 1975 *Ann. Rev. Nucl. Sci.* **25** 329
- [2] De Vries H, De Jager CW and De Vries C 1987 *Atomic Data and Nuclear Data Tables* **36** 495
- [3] Udías JM, Sarriguren P, Moya de Guerra E, Garrido E and Caballero JA 1993 *Phys. Rev. C* **48** 2731
- [4] Donnelly TW and Sick I 1984 *Rev. Mod. Phys.* **56** 461
- [5] Moya de Guerra E 1986 *Phys. Rep.* **138** 293; Moya de Guerra E 1980 *Ann. Phys. (N.Y.)* **128** 286
- [6] Al-Sammarraie AA, Sharrad FI, Yusof N and Kassim HA 2015 *Phys. Rev. C* **92** 034327
- [7] Wang Z, Ren Z, Dong T and Guo X 2015 *Phys. Rev. C* **92** 014309
- [8] Moya de Guerra E and Kowalski S 1980 *Phys. Rev. C* **22** 1308
- [9] Graca E *et al.* 1988 *Nucl. Phys. A* **483** 77
- [10] Sarriguren P, Graca E, Sprung DWL, Moya de Guerra E and Berdichevsky D 1989 *Phys. Rev. C* **40** 1414
- [11] Sarriguren P *et al.* 2019 *Phys. Rev. C* **99** 034325
- [12] T. Suda and H. Simon, *Prog. Part. Nucl. Phys.* **96**, 1 (2017)
- [13] Antonov AN *et al.* 2011 *Nucl. Inst. and Meth. A* **637** 60
- [14] Garrido E and Moya de Guerra E 2000 *Phys. Lett. B* **488** 68
- [15] Antonov AN *et al.* 2005 *Phys. Rev. C* **72** 044307
- [16] Dong T, Ren Z and Guo Y 2007 *Phys. Rev. C* **76** 054602
- [17] Roca-Maza X, Centelles M, Salvat F and Viñas X 2013 *Phys. Rev. C* **87** 014304
- [18] Liang T, Liu J, Ren Z, Xu C and Wang S 2018 *Phys. Rev. C* **98** 044310
- [19] Heyde K, Von Neumann-Cosel P and Richter A 2010 *Rev. Mod. Phys.* **82** 2365
- [20] Sarriguren P, Moya de Guerra E, Nojarov R and Faessler A 1994 *J. Phys. G* **20** 315
- [21] Berdichevsky D, Sarriguren P, Moya de Guerra E, Nishimura M and Sprung DWL 1988 *Phys. Rev. C* **38** 338
- [22] Moya de Guerra E, Sarriguren P, Caballero JA, Casas M and Sprung DWL 1991 *Nucl. Phys. A* **529** 68
- [23] Yennie DR, Ravenhall DG and Wilson RN 1954 *Phys. Rev.* **95** 500
- [24] Vautherin D 1973 *Phys. Rev. C* **7** 296
- [25] Chabanat E, Bonche P, Haensel P, Meyer J and Schaeffer R 1998 *Nucl. Phys. A* **635** 231
- [26] Antonov AN, Hodgson PE and Petkov IZ 1993 *Nucleon Correlations in Nuclei* (Springer-Verlag)
- [27] Kadrev DN, Antonov AN, Stoitsov MV and Dimitrova SS 1996 *Int. J. Mod. Phys. E* **5** 717
- [28] Blok HP and Heisenberg JH 1991 in *Computational Nuclear Physics 1: Nuclear Structure*, K. Langanke, J. A. Maruhn, S. E. Koonin (Eds.), Springer-Verlag.